Arch. Metall. Mater. **66** (2021), 2, 451-460

DOI: 10.24425/amm.2021.135878

YUE WANG[1,2*], PENG CHAI[1,2]

CHARACTERISTICS AND TENSILE-SHEAR PROPERTIES OF REFILL FSSW JOINT UNDER DIFFERENT PLUNGE DEPTHS IN 2060 ALUMINUM ALLOY

Refill friction stir spot welding (refill FSSW) was used to weld 3.2-mm-thick 2060 aluminum alloy. Joint formation, defect characteristics and tensile-shear property were analyzed. Results show that keyhole can be completely eliminated under different plunge depths. However, defects such as void, unconnected welding, hook can be observed under the plunge depths of 3.4-4 mm. The size of the overall void initially increased and then decreased with the increase of the plunge depth, while the void was the smallest under the plunge depth of 3.4 mm. The unconnected defect at the lap interface gradually shrank a welding line from obvious crack. Different hook morphologies were observed under different plunge depths. The tensile-shear load of joint increased with the increase of the plunge depth and was up to the largest under the plunge depth of 4 mm. All the tensile-shear specimens fractured along the lap interface. Compared with the void, the unconnected defect had a greater influence on the tensile-shear property.

Keywords: Refill friction stir spot welding, aluminum alloy, defect characteristics, tensile-shear properties

1. Introduction

Structural weight saving can be obtained by using aluminum alloys since the addition of element Li to aluminum alloys, aluminum lithium alloys, uniquely decreases an aluminum alloy's density while increases strength and modulus [1-2]. Aluminum lithium alloys are currently receiving considerable attention as a potential new generation of aerospace alloys [3-4]. Riveting is a prevalent method to connect lap structures. However, reduced efficiency due to drilling and increased weight of rivets are in urgent need of a new connection technique.

As a variant of friction stir spot welding (FSSW), refill friction stir spot welding (refill FSSW) developed by HZG (formerly known as GKSS) was a solid-state welding technology [5-6]. In addition to the advantages of FSSW, refill FSSW can successfully avoid keyhole, thereby attaining higher mechanical properties of refill FSSW joint [7-8]. Thus, the refill FSSW technology satisfies requirement for reduction in fuel consumption and cost in the aerospace industry for new materials and joining processes. Castro et al. [9] investigated the effect of welding parameters on 1.6-mm-thick 2198-T8 aluminum alloy joint's mechanical properties according to Taguchi method, and results show that rotational speed and plunge depth were responsible for more than 80% of strength variance. A similar result has been reported by Tier et al. [10]. The tensile-shear properties of 7B04-T74 aluminum alloy joint were dependent on hook geometry, location of alclad layer and hardness of stir zone (SZ) [11]. Cao et al. [12] reported that an increase in plunge depth increased the hook height and resulted in lower joint strength. Li et al. [13] pointed out that different plunge depths can change the hook morphologies, resulting in different effective sheet thickness and discrepant fracture modes of tensile-shear specimens.

There are limited literatures in refill FSSW joint for aluminum lithium alloys [9,14-15]. Shi et al. [14] and Yue et al. [15] conducted refill FSSW experiments of 2-mm-thick 2198-T8 aluminum alloy under different plunge depths and rotational speeds, respectively. For the 2060 aluminum lithium alloy, there is lack of related reports in refill FSSW joint [16]. This work is concentrated on the effect of the plunge depth on joint formation, defect characteristics and tensile-shear property of 3.2-mm-thick 2060 aluminum alloy refill FSSW joint.

2. Experiments

3.2-mm-thick 2060 aluminum alloy with the length of 150 mm and the width of 40 mm were used to obtain the refill FSSW joint in this study. Prior to welding the plates surfaces were

[1] BEIHANG UNIVERSITY, SCHOOL OF MECHANICAL ENGINEERING AND AUTOMATION, BEIJING 100191, P. R. CHINA
[2] BEIJING FSW TECHNOLOGY CO., LTD, AVIC MANUFACTURING TECHNOLOGY INSTITUTE, 100024, P. R. CHINA

* Corresponding author endlesswy@163.com

polished to wipe off the oxidations. Two plates were overlapped with 40×40 mm^2 and were joined in the center of the overlapped area, as shown in Fig. 1.

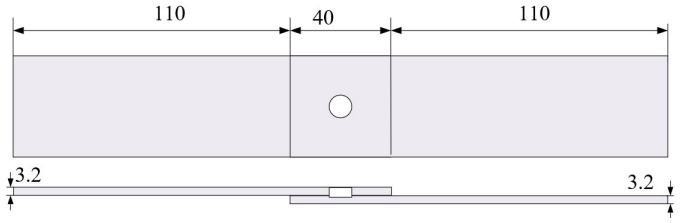

Fig. 1. Schematic of the tensile-shear specimen (all in mm)

Fig. 2 shows the refill FSSW robot equipment and the welding tool. This equipment consists of the robot body and welding head. The welding head designed and manufactured by Beijing FSW Technology Co., Ltd., can reach a maximum welding thickness of 4 mm. The outer diameters of the pin, sleeve and clamping ring were 6, 9 and 18 mm, respectively. The out walls of the sleeve and the pin were screw-like and radial grooves, respectively. The screw-like on the outer surface of the sleeve was aiming at making the material downwards. The outer surface of the pin does not directly contact with materials, and the radial grooves on outer surface of pin can decrease the contact area between the pin and the sleeve to reduce friction. After the components were assembled to the welding machine, radial run-out needed to be measured, and the tolerance should be in the range of 0~0.05 mm. The rotational speed was fixed as 2500 rpm, and plunge speed and refill speed were both 50 mm/min. Plunge depth was regarded as the variable, and it was in the range of 3.4-4 mm. According to different plunge sequence of the sleeve and the pin, the refill FSSW can be divided into two variants, including sleeve plunge and pin plunge variants [17]. In this study, sleeve plunge variant of refill FSSW was used to conduct experiments.

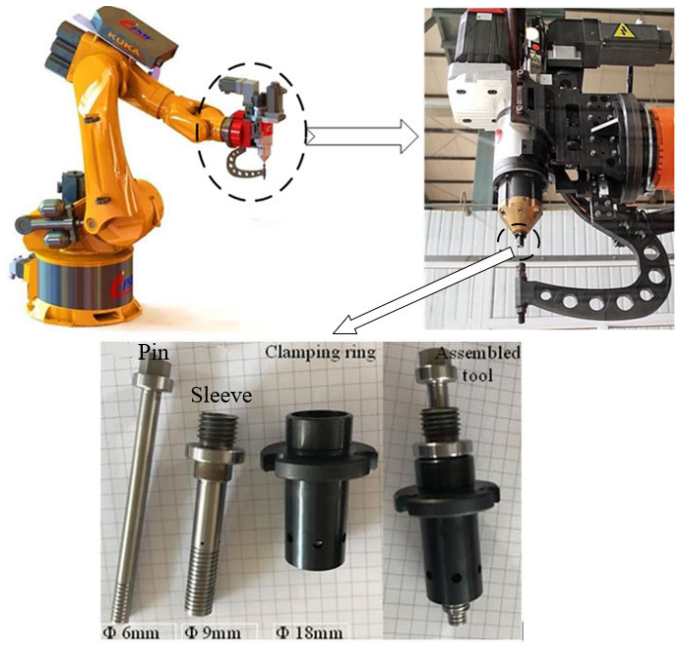

Fig. 2. Refill FSSW robot equipment and welding tool

The refill FSSW joint was cut along the center of the welding spot to obtain the cross section. This cross section was burnished, polished and etched using Keller's reagent. The cross section and microstructures were observed using an optical microscope (OM). The tensile-shear tests were performed three times for each rotational speed in accordance with the standard of ISO 6892-1-2009 "Metallic materials-Tensile testing-Part 1: Method of test at room temperature, and tensile-shear specimens". Furthermore, the fracture locations and surfaces were observed using the OM and an scanning electron microscope, respectively.

3. Results

3.1. Characterization of formation

Fig. 3 shows the cross sections of refill FSSW joints under different plunge depths. Like other aluminum alloys refill FSSW joints, the keyhole can be successfully refilled after welding. The cross section can be divided into SZ, heat-affected zone (HAZ), thermo-mechanically affected zone (TMAZ) and base

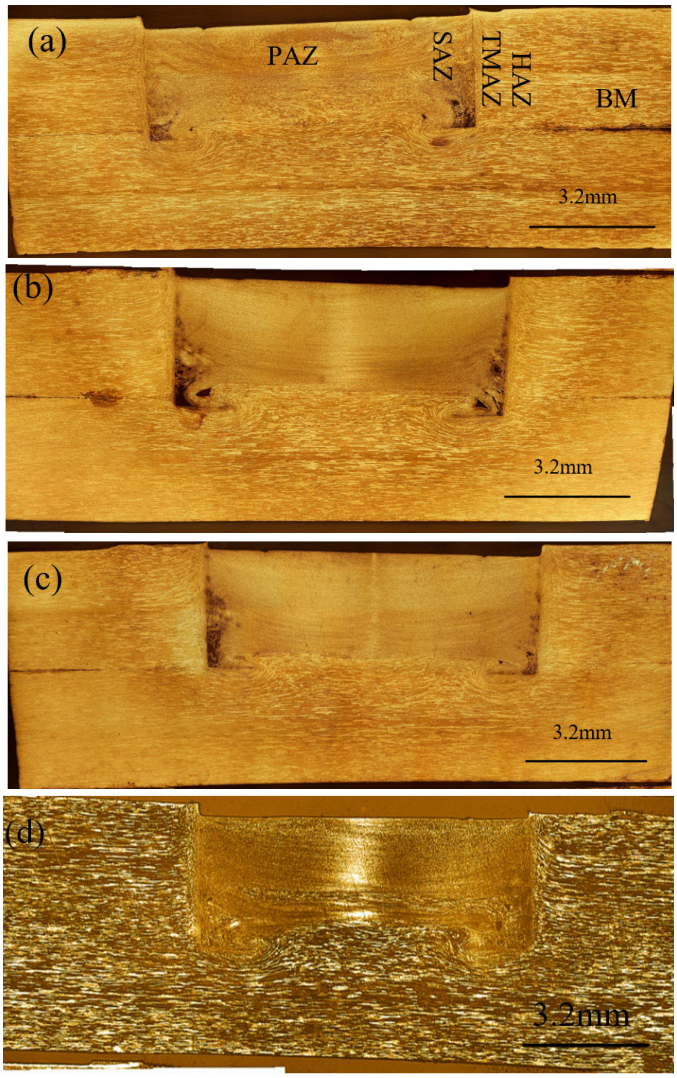

Fig. 3. Cross sections of refill FSSW joints under different plunge depths: (a) 3.4, (b) 3.6, (c) 3.8 and (d) 4 mm

material (BM). The SZ exhibits a U-shaped morphology, and it consists of pin-affected zone (PAZ) and sleeve-affected zone (SAZ) due to different stirring effects of the pin and the sleeve. Shen et al. [17] reported that the path along the sleeve retreating and lap interface were two significant interfaces to affect joint mechanical properties. These two regions are discussed in the following sections.

Fig. 4 shows the microstructure of the BM and HAZ. The BM plates were as-rolled condition, and their microstructures were elongated along the rolling direction, as shown in Fig. 4a. The EDX results of second-phase particles in the BM show that this second-phase particle was Al_2Cu. Because of thermal effect only, grains of the HAZ were coarsened, and second-phase particles were partially dissolved, as shown in Fig. 4b.

Fig. 5 shows the microstructures of the SAZ and TMAZ under different plunge depths. The fine and even grains in the SAZ were attributed to dynamic recrystallization due to violent stir and high temperature. Note that the second-phase particles were refined compared with those of the BM. Generally speaking, the larger plunge depth, the bigger grain size due to the longer welding time. However, grains of SAZ under the plunge depth of 3.4 mm were rather larger than those under the plunge depth of 4 mm. This can be explained by the over stirring resulting in broken grains again by the rotational tool [17], and the slip between the welding tool and material. During refill FSSW, heat was generated due to friction and plastic deformation [18], and the heat input varies with the welding parameters. The heat input increased to the maximum value when the plunge depth was up to 4 mm, and the peak temperature may approach or even reach the solidus temperature of material. In this elevated temperature, the viscosity of the material around the rotational tool was reduced, and thus the friction heat would not increase as the welding proceeded. Thus, the possible slip between the welding tool and material may occur. This slip could affect heat input and material flow during welding process, which in turn could influence the final microstructure and weld quality [19].

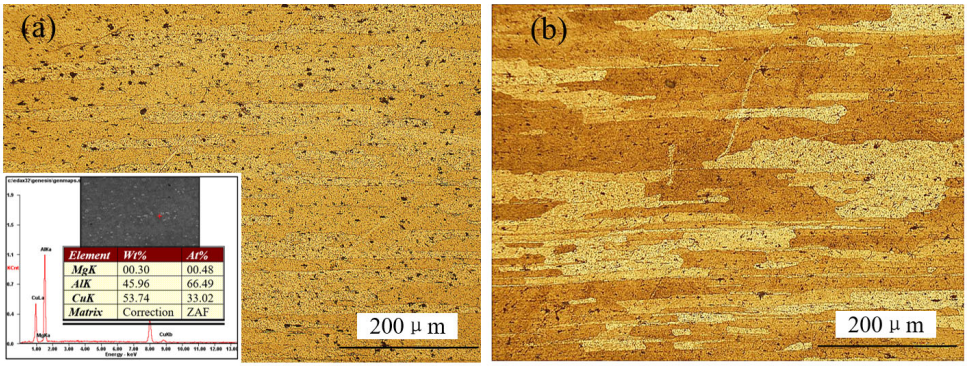

Fig. 4. Microstructures: (a) BM and (b) HAZ

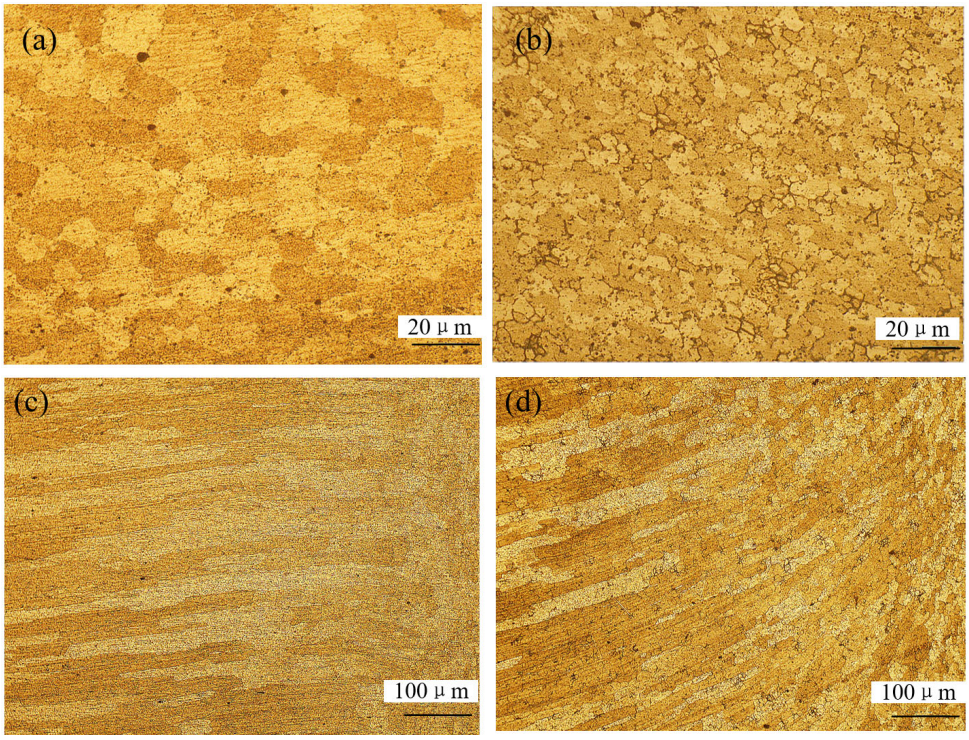

Fig. 5. Microstructures: (a) and (b) SZ, (c) and (d) TMAZ; (a) and (c) under plunge depth of 3.4 mm, (b) and (d) under plunge depth of 4 mm

Furthermore, the material may be broken under the violent stir of the rotational tool. Thus, the slip and the rapider rotation of the tool under the plunge depth of 4 mm were probably two reasons for the smaller grains.

The microstructures of the TMAZ were deformed due to moderate heat and driven by the rotational sleeve. Different plunge depths of the sleeve generated different deformation of microstructures in the TMAZ. The larger deformation degree was observed under the plunge depth of 4 mm, as shown in Fig. 5d.

3.2. Characterization of defects

Void occurred in each cross section, and it was located at the bottom of the SAZ. Fig. 6 shows the magnified views of the bottom of the SAZ of joints under different plunge depths. Furthermore, the voids at a certain cross section were asymmetrical, for example, Figs. 6a, 6c, 6e, 6g and Figs. 6b, 6d, 6f, 6h. The maximum values of void height of refill FSSW joint under plunge depth of 3.4 mm, 3.6 mm, 3.8 mm and 4 mm are

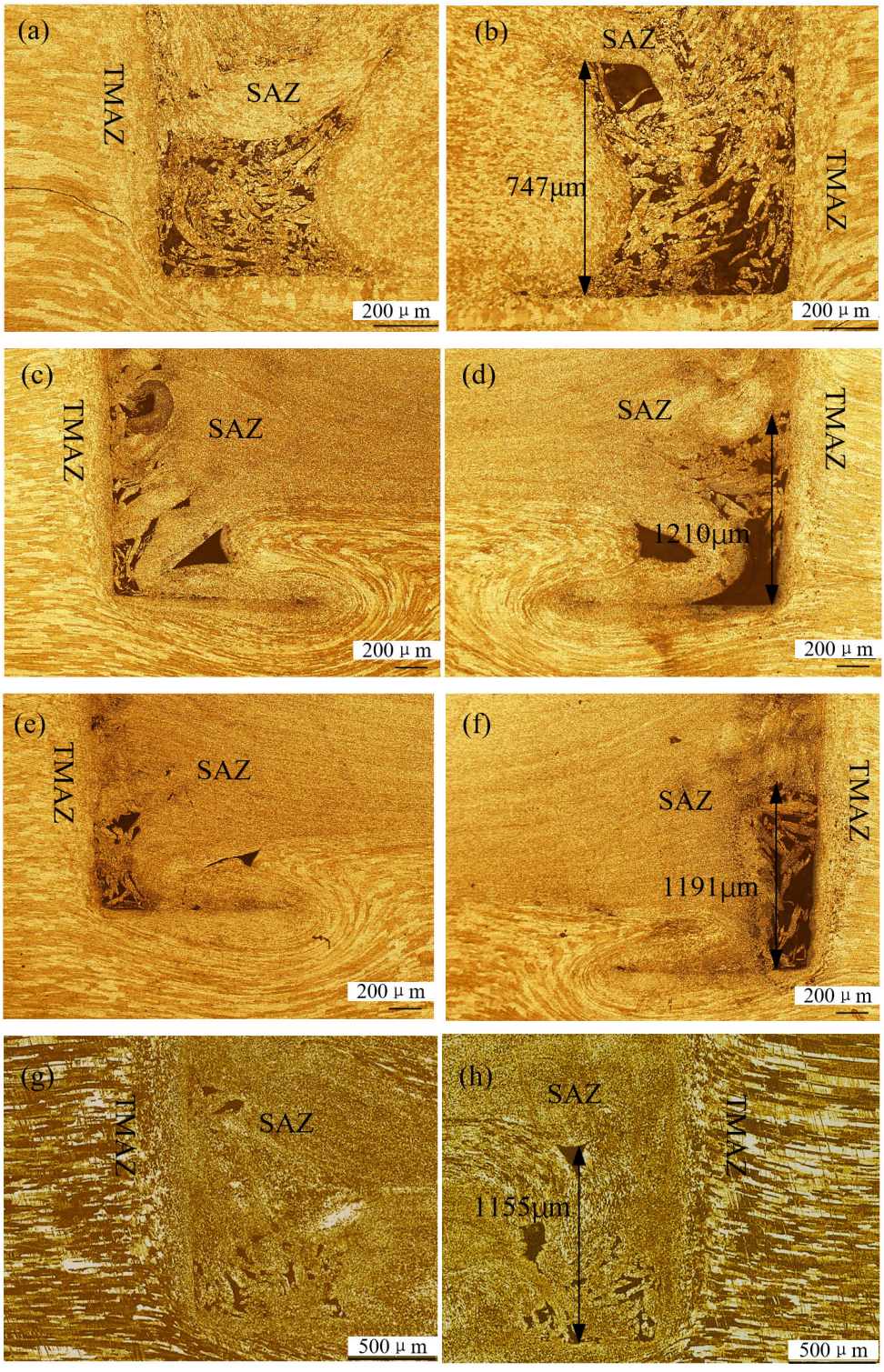

Fig. 6. Bottom of the SAZ of joints under different plunge depths: (a) and (b) 3.4, (c) and (d) 3.6, (e) and (f) 3.8 and (g) and (h) 4 mm

747 μm, 1210 μm, 1191 μm and 1155 μm, respectively, as shown in Fig. 6. The previous investigation pointed out that the void in the refill FSSW joint for 3.2 mm thick 2060 aluminum alloy cannot be completely eliminated at different rotational speeds fixing the plunge depth of 4 mm [16]. Yue et al. [15] reported that the void in the 2198 aluminum alloy refill FSSW joint was attributed to the insufficient refilling induced by material loss. Lowering the plunge depth can eliminate the void [15]. Shen et al. [18-19] reported that the void was associated with insufficient material flow.

The heat input increases with the increase of the plunge depth, and the viscosity of material around the sleeve becomes small. Generally speaking, the material fluidity becomes good under the large plunge depths, and the void is supposed to be reduced with increasing plunge depth. Note that the overall size of void initially increased and then decreased with the increment of the plunge depth, but the size of the whole void under the plunge depth of 4 mm was still larger than that of 3.4 mm. When the plunge depth increased to 3.6 mm, the size of the void increased sharply. However, it reduced slowly when the void continued to increase to 3.8 mm and 4 mm. Furthermore, under the small plunge depth, the void presented a large whole (Fig. 6a-6b), and the whole void was gradually shrunk to several small size with the increase of the plunge depth (Fig. 6c-6h). As mentioned above, the possible instability in the adhesion between the welding tool and material may occur under the high plunge depth. The viscosity of the material around the rotational tool is reduced and then the flow stress. Thus, this material exhibited a wide regime of flow instability, which led to the void defect in the joint under the high plunge depth.

Fig. 7 shows the hook morphology of joints under different plunge depths. The distance along the plate thickness from the top of the hook to the bottom of the hook is regarded as H, as shown in Fig. 7a. The values of H under the plunge depth of 3.4 mm, 3.6 mm, 3.8 mm and 4 mm are 272.37 μm, 91.40 μm, 130.23 μm and 86.04 μm, respectively.

At reported studies, the hook morphology was identical for refill FSSW joint at a certain material [20-23]. Shen et al. [20-21] pointed out the different hook morphologies were attributed to the different physical properties of materials. Note that different hook morphologies were obtained at this 2060 aluminum alloy refill FSSW joint.

When the plunge depth was 3.4 mm, the whole lap interface bent downward, and the bending height was largest, as shown in Fig. 7a. When the plunge depth was slightly increased to 3.6 mm, the bending lap interface can be divided into two parts, namely, near the SZ and away from the SZ. These two parts presented different bending morphologies. The region near the SZ continued to bend downward, and the lap interface away from the SZ bent upward, as marked in Figs. 7b-7d. The region of downward hook was in close proximity to the SZ, and this region had different physical properties with the material located at the TMAZ away from the SZ. Therefore, the above-mentioned two regions belonged to different affected zones, and they bent towards different directions. For the joint under the plunge depth of 3.4 mm, low heat input caused to small-area SZ and large viscosity of material, which resulted in small difference in viscosity of material between the TMAZ and the SZ. Thus, the whole lap interface under the plunge depth of 3.4 mm bent downward. The areas of SZ in the tip of the hook of joints under plunge depth

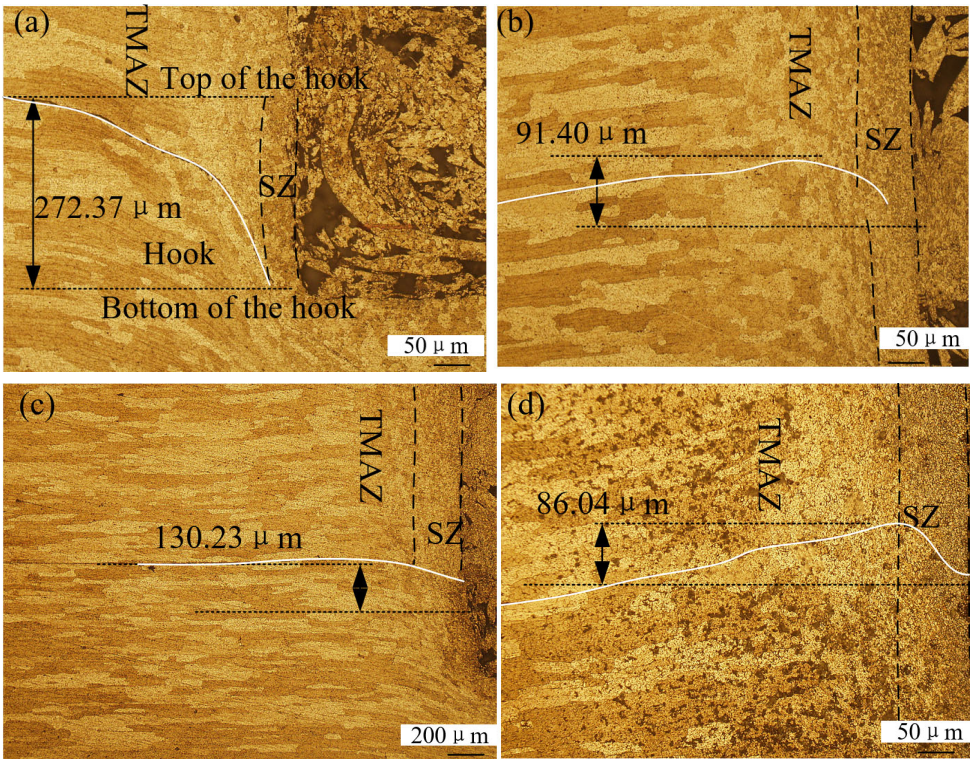

Fig. 7. Hook morphologies of joints under different plunge depths: (a) 3.4, (b) 3.6, (c) 3.8 and (d) 4 mm

of 3.4-4 mm (Figs. 7b-7d) were larger than that under plunge depth of 3.4 mm (Fig. 7a). Meanwhile, the heat input increased under the large plunge depth, which resulted in large difference in viscosity of material between TMAZ and SZ. The areas at the tip of the hook, namely, the SZ bent downward with the plunge of the sleeve at the plunging stage, and the areas away from the SZ, namely, the TMAZ cannot be completely driven by the SZ material due to large viscosity, and bent upward under the extrusion of SZ material. With the increase of the plunge depth the numerous materials of SZ was used to fill keyhole, and thus less material to squeeze the lap interface. Thus, the large void under the plunge depth of 4.0 mm corresponded to the small value of H.

Fig. 8 shows the lap interfaces below the PAZ of joints under different plunge depths. At the plunging stage, the sleeve plunged into the plates. Hence, the material of the lap interface below the pin was regarded as a whole and then was not stirred but was completely squeezed into the space which was inside the sleeve and just right below the pin under the extrusion of the sleeve. At the refilling stage, this part of the material was returned to the welding spot under the extrusion of the pin. On the whole, the lap interface below the pin mainly occurred diffusion bonding. When the plunge depth was small, welding time was short, and then the lap interface was not completely welded. This defect was regarded as unconnected defect, as shown in Fig. 8a.

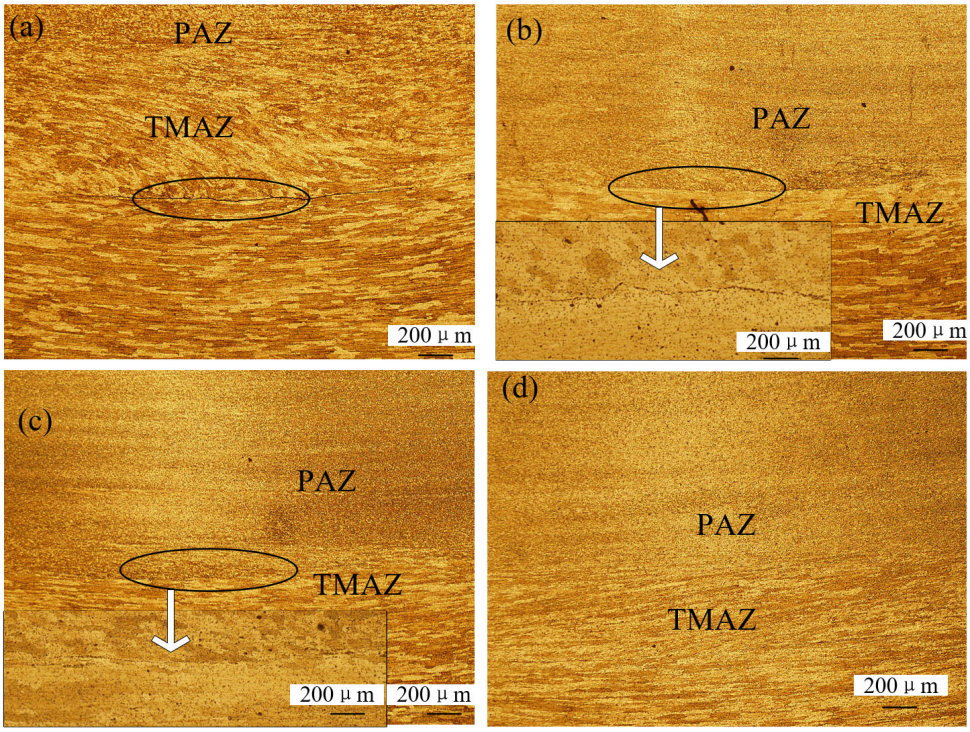

Fig. 8. Lap interfaces of joints under different plunge depths: (a) 3.4, (b) 3.6, (c) 3.8 and (d) 4 mm

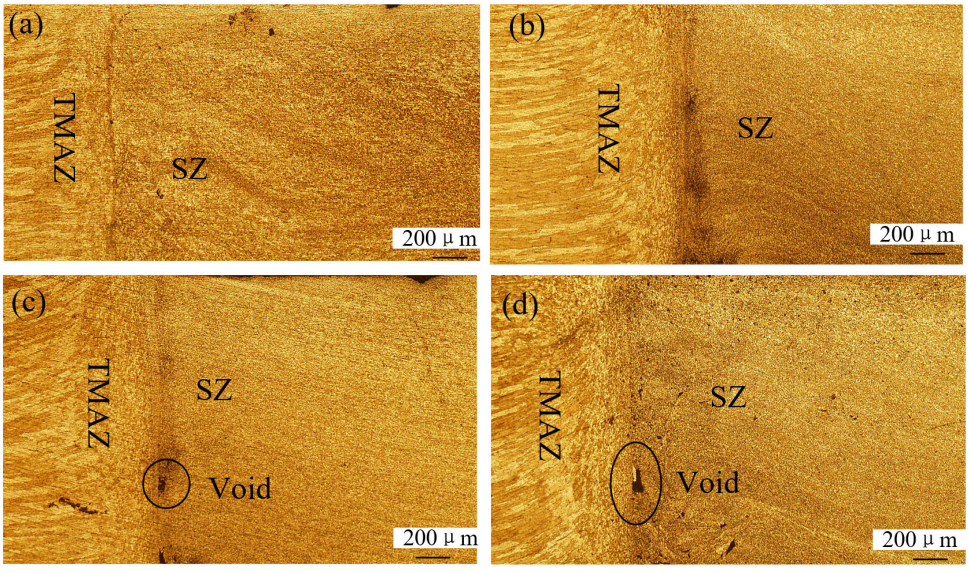

Fig. 9. SAZ/TMAZ interfaces under different plunge depths: (a) 3.4, (b) 3.6, (c) 3.8 and (d) 4 mm

With the increase of the plunge depth, the unconnected defect shrank a welding line (Figs. 8b and 8c). When the plunge depth increased to the 4 mm, the unconnected defect disappeared, and the lap interface was welded.

Besides the lap interface, the welding quality of the SAZ/TMAZ interface was also a critical factor to decide the joint quality. Fig. 9 shows the SAZ/TMAZ interfaces of joint under different plunge depths. There were large differences in the microstructures. However, the lack of mixing and cracks were not observed in this interface. Void occurred in this interface under the plunge depths of 3.8 and 4 mm.

3.3. Tensile-shear properties of joint

Fig. 10 shows the typical load-displacement curves and tensile-shear load of joints under different plunge depths. The curves almost increased linearly with increasing displacement within a certain range, and then the slopes of the curves gradually decreased. The load sharply decreased as soon as it reached the maximum. The mean tensile-shear load under each welding parameter increased with the increase of the plunge depth. The minimum value of mean tensile-shear load was only 7.23 kN, and the joint is obtained at the plunge depth of 3.4 mm. When the plunge depth increased to 4 mm, the mean tensile-shear load of joint is up to the maximum of 10.64 kN. All the tensile-shear load was averaged by three values.

In this study, the tensile-shear load of joint increased with the increase of the plunge depth in the range of 3.4-4 mm, and the maximum value was achieved under the limit of the equipment. In this condition, the plunge depth of 4 mm and rotational speed of 2500 rpm can be used to conduct experiments combined with primary experimental results [16]. If the plunge depth of the welding equipment is greater than 4 mm, the plunge depth can be further optimized at the rotational speed of 2500 rpm.

For other series of aluminum alloys whose thickness was less than or equal to 2 mm, various fracture modes were obtained under different welding parameters [13,24-25]. Li et al. [13] investigated the fracture mechanism of 2024 aluminum alloy refill FSSW joint, and three different types of fracture modes were obtained, including shear fracture, shear-plug fracture and plug fracture. Kubit et al. [24] and Zhou et al. [25] only obtained two of these three types of fracture modes for (1.6 + 0.8) mm thick 7075-T6 aluminum alloy and (2 + 2) mm thick 6061-T6 aluminum alloy refill FSSW joints, respectively. In this study, the tensile-shear specimens under different plunge depths fractured along the lap interface of the upper and lower sheets. This study is focused on the tensile-shear specimens with the smallest and largest loads, as shown in Figs. 11a and 12a.

Figs. 11 and 12 show the macro- and micro-photographs of fractured tensile-shear specimens under the plunge depths of 3.4 mm and 4 mm, and the tensile-shear loads of joints in Figs. 11 and 12 were 7.01 kN and 10.88 kN, respectively. The selected minimum value was lower than the mean value of joint under the plunge depth of 3.4 mm, and the maximum value was larger than the mean value of joint under the plunge depth of 4 mm.

Regions I, II and III in the Figs. 11a and 12a represented the fracture surfaces at the boundary between the SAZ and the PAZ, the PAZ and the SAZ, respectively. The lap interface can be joined well under the proper plunge depth. When the plunge depth was small, the insufficient heat input made the lap interface at the PAZ weak. As mentioned above, this lap interface was connected by diffusion. Note that the fracture surface was smooth, which indicated that the lap interface was revealed under the extra load. From the magnified view in Fig. 11e, there was no characteristic of ductile joining. When the plunge depth reached 4 mm, the heat input was sufficient to connect lap interface. The tear edge was obvious in region II (Fig. 12e), indicating ductile fracture. The material in the boundary between the PAZ and the SAZ flowed adequately under the high-speed rotation of the pin and the sleeve at different plunge depths. There were obvious ductile fracture characteristics in Region I in the magnified views (Figs. 11c and 12c).

The material at the bottom of the SAZ was incompletely plastized under the plunge depth of 3.4 mm leading to the poor flowability, and thus the volume defect of void was generated blocking the close contact between the upper and lower plates. Due to the plunge of the sleeve the indentation on the lower sheet

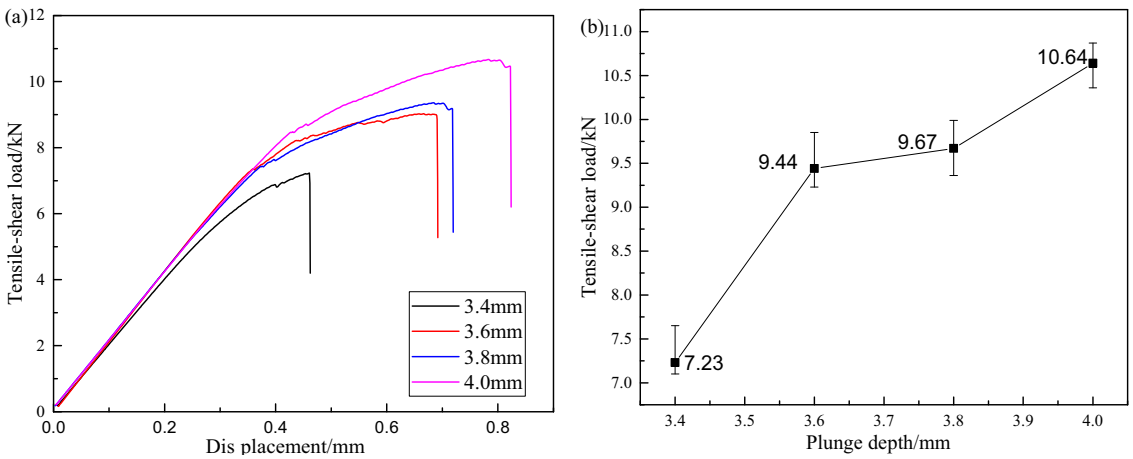

Fig. 10. Tensile-shear properties of joints under different plunge depths: (a) load-displacement curves and (b) tensile-shear load

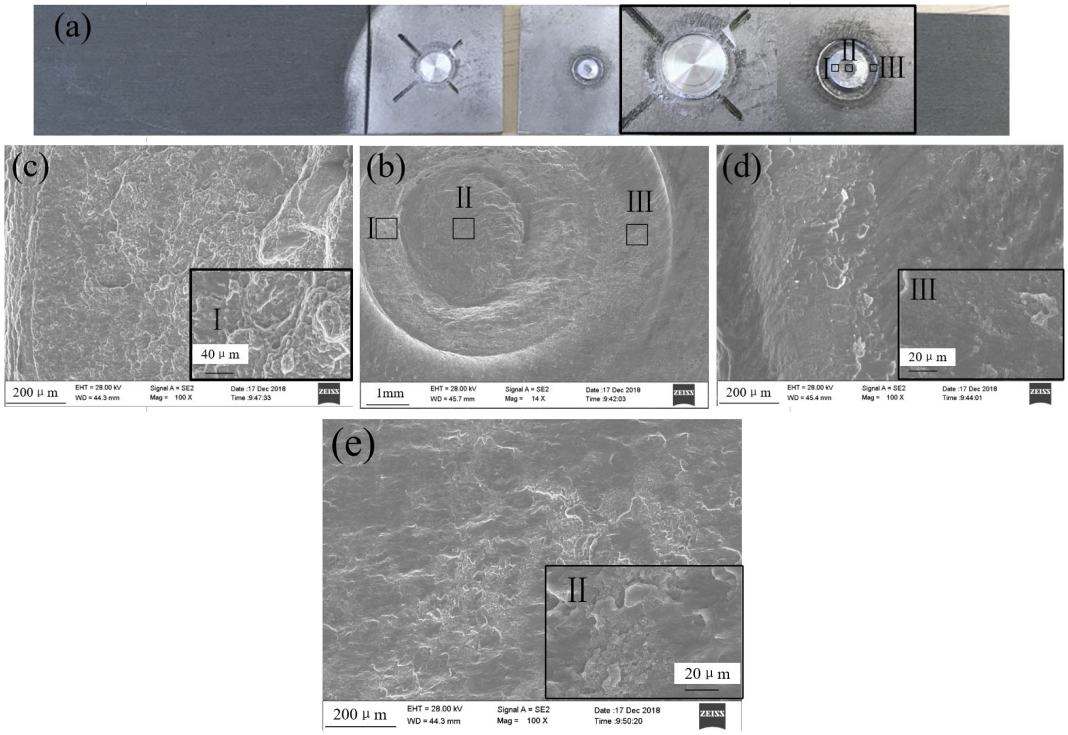

Fig. 11. Fracture surface morphologies of tensile-shear specimen under plunge depth of 3.4 mm: (a) macrostructure, (b) partial enlarged views of (a), (c) Region I, (d) Region II and (e) Region III

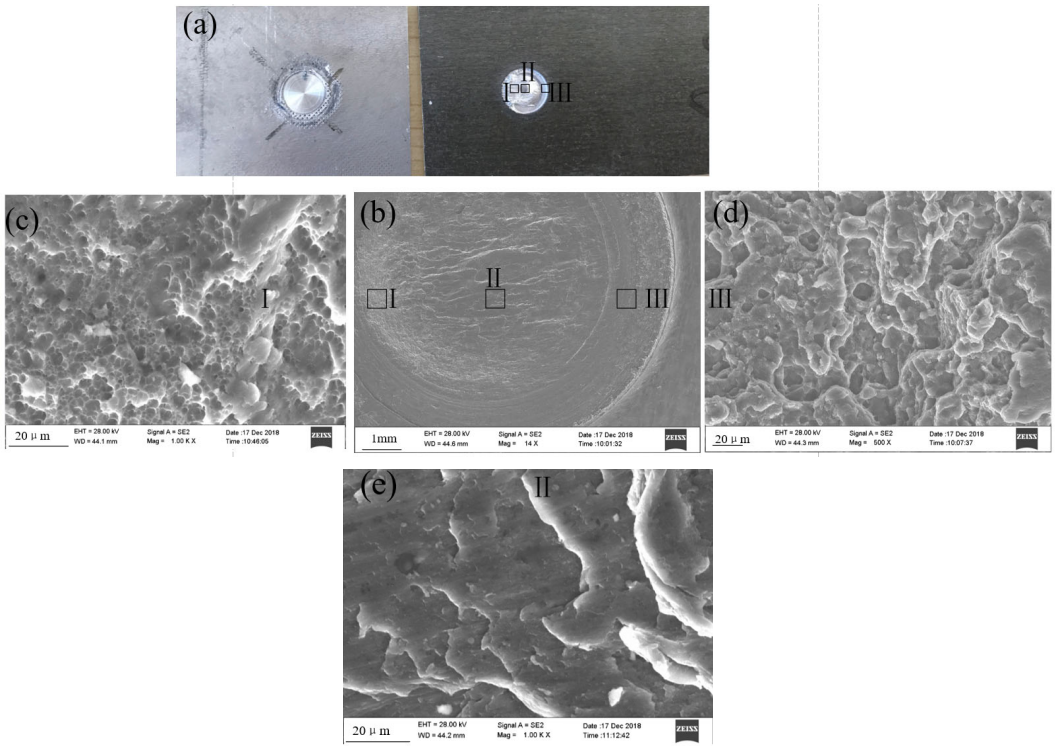

Fig. 12. Fracture surface morphologies of tensile-shear specimen under plunge depth of 4 mm: (a) macrostructure, (b) partial enlarged views of (a), (c) Region I, (d) Region II and (e) Region III

was obvious from the fracture surface. In the magnified view of Region III, the smooth and flat surface was observed in Fig. 11d. Increasing the plunge depth to 4 mm, the size of the whole void at the bottom of the SAZ increased, but the single void was decreased. Meanwhile, the lap interface was connected well. Consequently, the joining strength of the lap interface enhanced, which results in the apparent tear edge (Fig. 12d).

Fig. 13 shows the fracture locations of tensile-shear specimens in Figs. 11a and 12a. Obviously, the refill FSSW joint under different plunge depths fractured along the lap interface.

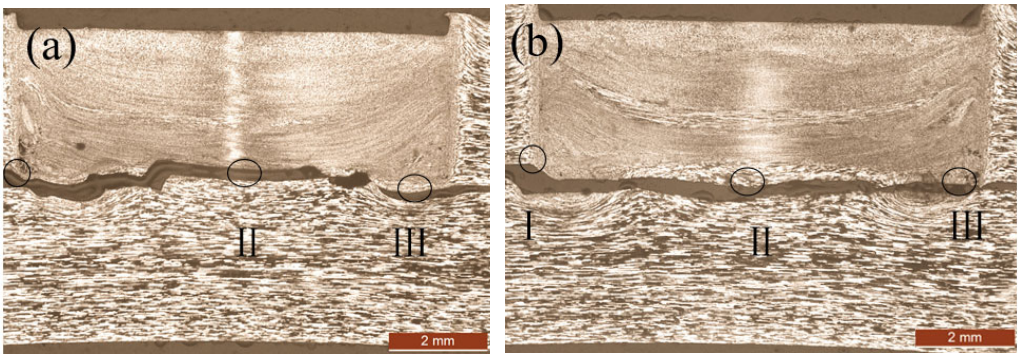

Fig. 13. Fracture locations of joints under different plunge depths: (a) 3.4 mm and (b) 4 mm

The presented fracture modes were typical for the conducted experiments, and every sample at the same welding condition fractured along the same path.

The void belongs to volume defect, and it weakens the effective working section, which can remarkably decrease joint strength. For the unconnected welding similarly to crack, its notch is sharp and the length-width ratio of crack is large. From the magnified views of the lap interface of joints under different plunge depths (Fig. 8), the unconnected defect was obvious under the plunge depths of 3.4 mm. When the plunge depth increased to 4 mm, the lap interface was well joined. The unconnected lap interface increased the stress concentration and decreased the connecting area. During the external load, crack initiated from the bending hook and the tip of the unconnected lap interface, and directly propagated along the lap interface for the joint with the unconnected lap interface (Fig. 13a).

For the joint only with void under the plunge depth of 4 mm, they had small stress concentration points and crack extending path, and the crack initiated from hook propagated along the area below the lap surface, as shown in Fig. 13b. The refill FSSW joint with good connected lap interface had larger tensile-shear load than joints with unconnected lap interface (Fig. 10). Compared with the void in the SAZ/TMAZ interface, the crack in the lap interface had a more negative effect on the joint quality.

In terms of force, the side wall of the welding spot bears the tensile stress σ due to the relationship between force and reaction force under the external load. The lap interface is subjected to shear stress τ, and the shear area is the lap interface. Fig. 14 shows the stress model of refill FSSW joint under external load. In this study, the shear area was only the PAZ area at the lap interface because the SAZ was not welded well. The void at the bottom of the SAZ not only increased the crack initiation, but also decreased the load-bearing area of joint.

Thus,

$$\sigma = F/(d_1 h)$$

$$\tau = F / \left(\pi \left(\frac{d_2}{2} \right)^2 \right)$$

Thereinto, d_1 and d_2 represented the diameters of the sleeve and the pin; h represented the connected height along the plate thickness. Table 1 shows the values of h under different plunge depths. Note that the size of the void increases with the increase of the plunge depth but the connected area does not decrease. Furthermore, the joint under the plunge depth of 4 mm with the largest void have the largest tensile-shear load.

TABLE 1

Values of h of joints under different plunge depths

Plunge depth, mm	3.4	3.6	3.8	4
Height of void, mm	0.747	1.21	1.191	1.155
Joining height/h, mm	2.653	2.39	2.609	2.845

When $\tau = \sigma$,

$$F/(d_1 h) = F / \left(\pi \left(\frac{d_2}{2} \right)^2 \right) \quad (1)$$

Bring $d_1 = 9$ mm and $d_2 = 6$ mm into formula (1), $h = \pi$ mm.
When $h > \pi$ mm, $\tau > \sigma$;
When $h < \pi$ mm, $\tau < \sigma$.

From Table 1, the values of h of joints under different plunge depths were smaller than π. Thus, the tensile stress in the side wall was larger than shear stress at the lap interface if the test plates after welding were homogeneous. However, the

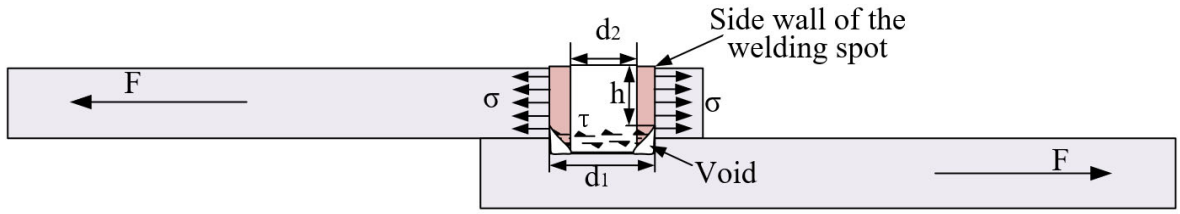

Fig. 14. Stress model of joint under the external load

connection status of the lap interface after welding was different from that of the path sleeve retreating [13]. The analysis of the force and fracture location in Fig. 13b further indicates that the lap interface had a significant influence on the tensile-shear properties of refill FSSW joint. Although the lap interface with the good connection under the plunge depth of 4 mm increased the tensile-shear load, the increasing degree of the connectivity of the lap interface did not change the fracture position of joint. Thus, the increase of the tensile-shear load of refill FSSW joint can be achieved by increasing the connection degree of the lap interface.

5. Conclusions

1. Keyhole was completely refilled in 2060 aluminum alloy joints under different plunge depths. Compared with the grains under the plunge depth of 3.4 mm, the grains in SAZ were refiner and deformation degree of grains in TMAZ was larger under the plunge depth of 4 mm.
2. The void was not eliminated when the plunge depth was in the range of 3.4-4 mm. The size of the overall void initially increased and then decreased, but the void in the joint under the plunge depth of 4 mm was still larger than under the plunge depth of 3.4 mm. Furthermore, the single void was shrunk to several small void with the increase of the plunge depth.
3. The unconnected defect was obvious under the smallest plunge depth. It gradually reduced to a connecting line when the plunge depth reached 3.8 mm, and disappeared under the plunge depth of 4 mm.
4. The tensile-shear load of joint in the range of the plunge depth of 3.4 - 4 mm increased with the increase of the plunge depth. All the tensile-shear specimens fractured along the lap interface. The unconnected defect was much more deleterious to joint strength than the void.

Acknowledge

This work is supported by the National Natural Science Foundation of China (No. 51705339) and Aeronautical Science Foundation of China (No. 20171125002).

REFERENCES

[1] R.G. Buchheit, J.P. Moran, G.E. Stoner, Mater. Sci. Forum. **2**, 1641 (2000).
[2] R.J. Bucci, R.C. Malcolm, E.L. Colvin, S.J. Murtha, R.S. James, NSWS Final Report **15**, 89 (1989).
[3] A.K. Vasuhevan, E.A. Ludwiczak, S.F. Baumann, R.D. Doherty, M.M. Kersker, Mater. Sci. Eng. **72**, 25(1985).
[4] R.J. Rioja, J. Liu, Metall. Mater. Trans. A. **43**, 3325 (2012).
[5] S.T. Amancio-Filho, A.P. Camillo, L. Bergmann, Mater. Trans. **52**, 985 (2011)
[6] M.K. Kuleki, Arch. Metall. Mater. **59** (1), 221-224 (2014).
[7] P. Lacki, W. Wieckowski, P.Wieczorek, Arch. Metall. Mater. **60** (4), 2297-2306 (2015).
[8] P. Lacki, A. Derlatka, T. Galaczynski, Arch. Metall. Mater. **62** (1), 443-449 (2017).
[9] D.C.C. Caroline, P.A. Henrique, D.A.N. Guedes, D.S.J. Fernandes, Int. J. Adv. Manuf. Tech. **99**, 1927 (2018).
[10] M.D. Tier, T.S. Rosendo, J.F.D. Santos, N. Huber, T.R. Strohaecker, J. Mater. Process Tech. **213**, 997 (2013).
[11] Y.Q. Zhao, H.J. Liu, S.X. Chen, Z. Lin, J.C. Hou, Mater. Des. **62**, 40 (2014).
[12] J.Y. Cao, M. Wang, L. Konga, L.J. Guo J. Mater. Process Tech. **230**, 254 (2016).
[13] Z.W. Li, S.D. Ji, L. Ma, P. Chai, Y.M. Yue, Int. J. Adv. Manuf. Tech. **86**, 1925 (2016).
[14] Y. Shi, Y.M. Yue, Zhang LG, S.D. Ji, Y. Wang, T. Indian I. Metals. **71**, 139 (2017).
[15] Y.M. Yue, Y. Shi, S.D. Ji, Y. Wang, Z.W. Li, J. Mater. Eng. Perform. **26**, 5064 (2017).
[16] P. Chai, Y. Wang, Met. Mater. Int. **6**, 1574 (2019).
[17] Y. Wang, P. Chai, H. Ma, X.M. Cao, Y.H. Zhang, J. Mater. Sci. **55**, 358 (2020).
[18] J.Y. Cao, M. Wang, L. Kong, Y.H. Yin, L.J. Guo. Int. J. Adv. Manuf. Technol. **89**, 2129 (2017).
[19] J. Wang, J. Su, R.S. Mishra, R. Xu, J.A. Baumann. Wear **321**, 25-32 (2014).
[20] Z.K. Shen, X. Yang, Z. Zhang, L. Cui, T. Li, Mater. Des. **44**, 476 (2013).
[21] Z.K. Shen, X.Q. Yang, S. Yang, Z.H. Zhang, Y.H. Yin, Mater. Des. **54**, 766 (2014).
[22] S.D. Ji, Y.X. Wang, J. Zhang, Z.W. Li, Int. J. Adv. Manuf. Technol. **90**, 717 (2016).
[23] B. Parra, V.T. Saccon, N.G.D. Alcântara, T. Rosendo, J.F. Santos, Tecnologia Em. Metalurgia Materiais E. Mineralo. **8**, 184 (2011).
[24] A. Kubit, M. Bucior, D. Wydrzyński, T. Trzepieciński, M. Pytel, Int. J. Adv. Manuf. Technol. **94**, 4479 (2018).
[25] L. Zhou, L.Y. Luo, T.P. Zhang, W.X. He, Y.X. Huang, J.C. Feng, Int. J. Adv. Manuf. Technol. **92**, 3425 (2017).